Hybrid Optimal Control Approach to Commercial Aircraft Trajectory Planning

M. Soler,* A. Olivares,† and E. Staffetti†

Universidad Rey Juan Carlos, 28933 Madrid, Spain

* Ph.D. Candidate, Department of Statistics and Operations Research,School of Telecommunication Engineering. Student Member AIAA.

† Associate Professor, Department of Statistics and Operations Research, School of Telecommunication Engineering.

Nomenclature

C_D	=	coefficient of drag
C_{D_0}	=	coefficient of parasite drag
C_L	=	coefficient of lift
$C_{L_{max}}$	=	maximum coefficient of lift
$C_{Tc,4}$	=	first thrust temperature coefficient
$C_{V_{min}}$	=	minimum speed coefficient
D	=	drag force, $0.5\rho V^2 S C_D$
G_t	=	temperature gradient on maximum altitude
G_W	=	mass gradient on maximum altitude
g	=	acceleration due to gravity
h	=	altitude
h_{M_0}	=	maximum operating altitude
h_{max}	=	maximum altitude at maximum takeoff weight under Instrument Society of America conditions
h_u	=	maximum dynamic altitude
K	=	coefficient of induced drag
L	=	lift force, $0.5\rho V^2 S C_L$
M	=	Mach number
M_{M0}	=	maximum operating Mach number

m	=	mass
$\dot{m}$	=	fuel flow
m_{max}	=	maximum mass (maximum takeoff weight)
m_{min}	=	minimum mass (operating empty weight)
$\dot{m}_{min}$	=	minimum fuel flow
S	=	reference wing surface area
T	=	thrust
T_{max}	=	maximum thrust
V	=	true airspeed
V_{CAS}	=	calibrated airspeed
V_{M_0}	=	maximum operating calibrated airspeed
V_{stall}	=	stall speed
x	=	distance
α	=	angle of attack
ΔT_{ISA}	=	temperature deviation from International Standard Atmosphere
η	=	thrust specific fuel flow
γ	=	flight-path angle
ρ	=	atmospheric density

I. Introduction

A SUBSTANTIAL change in the current air traffic management (ATM) paradigm is needed, because this system (which is responsible for sustainable, efficient, and safe operations in civil aviation) is reaching the limit of its capabilities. Its capacity, efficiency, environmental impact, and flexibility should be improved to accommodate airspace users' requirements.‡ The need to fit aircraft trajectories to ATM system requirements makes them difficult to be optimized, and therefore suboptimal flight profiles are generally being flown.

With this aim, this paper presents an approach to commercial aircraft optimal trajectory generation in which different flight phases and operational procedures can be combined so that a single optimal control problem is solved. The coupling of these discrete flight phases with the continuous aircraft dynamics results in a hybrid system [1–3]. In particular, the flight of an aircraft intrinsically has the characteristics of a controlled switched dynamic system [4,5]. Indeed, several flight modes can be distinguished for climbing, cruising and descent, each with an associated dynamic model and a set of path constraints.

On the whole, it is difficult to find all the components for the solution to hybrid optimal control problems because the optimal sequence of discrete states is very difficult to determine. In our case, the phase sequence is given, but optimal switching times must be determined. Problems with known phase sequence have been frequently solved in aerospace engineering as multiphase problems [6–9], most of them were solved using pseudospectral methods [10,11]. However, none of these works focused on commercial aircraft. Pseudospectral knotting methods have been developed for solving multiphase optimal control problems (see, for instance,

[12]). Such knotting methods need knotting conditions to connect adjacent phases. In our approach we convert the hybrid optimal control into an equivalent, conventional optimal control problem, making the unknown switching times part of the state by using a method similar to those presented in [13,14]. In this way, we do not need to connect adjacent phases with linkage constraints. The resulting optimal control problem is then solved using a Simpson collocation method [15,16].

The fundamental prior research work on aircraft trajectory optimization within the current ATM concept was presented in [17]. The flight of an aircraft was modeled as a collection of phases and procedures in which continuity of the state variables was imposed in order to link phases, permitting discontinuities in control variables and flight-path angle. Moreover, concatenating optimal phase-by-phase solutions does not lead to an overall optimal trajectory. Recently, in [18], a method to compute overall optimal trajectories has been presented. Modeling the actual ATM paradigm, as in [18], enforces the specification of two operative procedures per phase, for instance, to climb with constant V_{CAS} and constant throttle setting, or to perform a steady cruise: i.e., with constant Mach and constant altitude. On the contrary, in this work we set only one operative procedure per phase: e.g., to climb with constant V_{CAS}, or to cruise at constant altitude as in [19]. This assumption increases the complexity of aircraft dynamic equations, but also gives more room for planning more efficient flight profiles.

An application of our method to the trajectory optimization of a vertical-point-mass model of an Airbus A-320 is reported. The results show the efficiency of our approach.

‡Single European Sky ATM Research (SESAR) ATM Master Plan is available online at http://www.eurocontrol.int/sesar [retrieved 15 March 2010].

II. Optimal Control Problem

A switched dynamic system is composed of a set of dynamic systems:

$$\dot{x} = f_k[x(t), u(t), t], \qquad k \in \{1, 2, \ldots, N_D\} \qquad (1)$$

where x represent the n-dimensional state vector, and the set $\{1, 2, \ldots, N_D\}$ represents the different dynamic systems. To control a switched dynamic system, both an m-dimensional control input $u(t)$ and a switching sequence σ have to be specified. We suppose that the set of admissible control inputs is a set of piecewise-continuous functions in $t \in [t_I, t_F]$. A switching sequence in $[t_I, t_F]$ is defined as the timed sequence of $N + 1$ active dynamic systems:

$$\sigma = [(t_I, k_I), (t_1, k_1), \ldots, (t_N, k_N)] \qquad (2)$$

where $0 \leq N < \infty$, $t_I \leq t_1 \cdots \leq t_N \leq t_F$, and $k_j \in \{1, 2, \ldots, N_D\}$. In this sequence, the pair (t_j, k_j) indicates that at time t_j the dynamic equation of the switched system changes from k_{j-1} to k_j, with $t_0 = t_I$ and $t_{N+1} = t_F$. As a consequence, in the time interval $[t_j, t_{j+1}]$ the system evolution is governed by the dynamic equation k_j. In the interval $[t_N, t_F]$ the active dynamic system is k_N.

The pairs (t_j, k_j) can be classified in two categories: those corresponding to autonomous switches and those corresponding to controlled switches. For instance, an autonomous switch may occur when the aircraft reaches a prescribed altitude. On the contrary, a controlled switch takes place in response to control inputs established by the solution to the optimal control problem. In this work, we assume that the sequence of phases is given by a flight profile; i.e., the untimed sequence of active systems $\zeta = (k_I, k_1, \ldots, k_N)$ is known.

Fig. 1 Relation between scaled time τ and real (unscaled) time t.

$t_F = t_{N+1} = 1$. The first step is to introduce the new state variables $x_{n+1}, \ldots, x_{n+N}$, which correspond to the switching times t_i for $i \in \{1, 2, \ldots, N\}$: i.e., $x_{n+i} = t_i$, with $\dot{x}_{n+i} = 0$.

We then introduce the new independent variable τ. The relation between τ and t changes on each interval $[t_i, t_{i+1}]$. We establish piecewise-linear correspondence between time t, and the new independent variable τ, so that for every chosen fixed point τ_i $(i = 1, \ldots, N)$, t equals t_i. Any monotonically increasing sequence of N numbers on interval $[0, 1]$ could be used. We set $\tau_i = i/(N + 1)$. As a result, we obtain the following expression:

$$t = \begin{cases} (N + 1)x_{n+1}\tau, & 0 \leq \tau \leq \frac{1}{N+1} \\ (N + 1)(x_{n+i+1} - x_{n+i})\tau + (i + 1)x_{n+i} - ix_{n+i+1}, & \frac{i}{N+1} < \tau \leq \frac{i+1}{N+1} \\ (N + 1)(1 - x_{n+N})\tau + (N + 1)x_{n+N} - N, & \frac{N}{N+1} < \tau \leq 1 \end{cases}$$

The hybrid optimal control problem can be stated as follows: Consider the switched dynamic system (1) whose state and control variables are subjected to a set of equality and inequality constraints:

$$g_k[x(t), u(t), t] = 0, \qquad h_k[x(t), u(t), t] \leq 0$$
$$k \in \{1, 2, \ldots, N_D\} \qquad (3)$$

Given an initial state $x(t_I)$, a final state $x(t_F)$, a time interval $[t_I, t_F]$, and a prescribed untimed sequence of active dynamic systems ζ, find a piecewise-continuous input $u(t)$, the switching instants $(t_1, \ldots, t_N)$, and the corresponding piecewise smooth trajectory $x(t)$ between $x(t_I)$ and $x(t_F)$ that fulfill Eqs. (1) and (3), and minimize

$$J = \phi[x(t_F)] + \int_{t_I}^{t_F} L[x(t), u(t), t]\, dt \qquad (4)$$

The final time t_F may be fixed in advance or left free. We assume that f_k, g_k, h_k, and ϕ are smooth enough functions.

This hybrid optimal control problem is converted into an optimal control problem, making the unknown switching times part of the state and introducing a new independent variable with respect to which the switching times are fixed [13,14]. In this reformulated problem, there is a linear relation between the new variable and time, but the slope of this linear relation changes on each interval between two switches. These slopes, which are part of the solution to the optimal control problem, are actually time scaling factors that determine the optimal switching times (see Fig. 1).

As previously stated, the number of switches N and the sequence of discrete states ζ, which the system evolves through, are known. Without loss of generality, we can assume that $t_I = t_0 = 0$ and
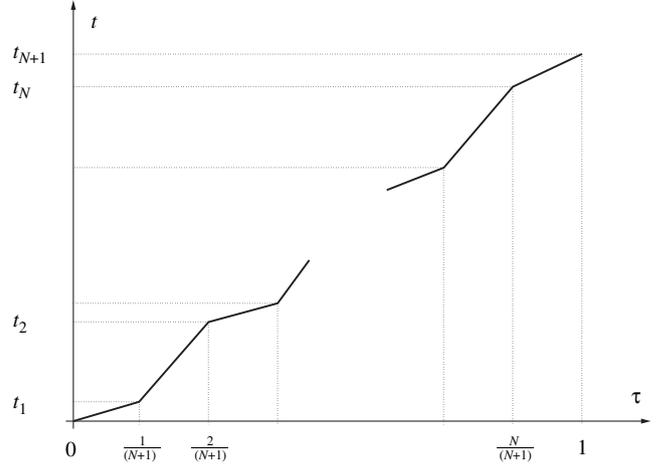
By introducing the new independent variable τ, the evolution equation on the interval $[t_i, t_{i+1}]$ given by Eq. (1) becomes

$$x' = (N + 1)(x_{n+i+1} - x_{n+i})\hat{f}_i(x, u, \tau) \qquad (5)$$

where prime denotes the derivative of $(\cdot)$ with respect to the new independent variable τ and

$$\hat{f}_i(x, u, \tau) = f_i(x, u, t(\tau))$$

Let $\hat{x}$ be the extended state vector

$$\hat{x} = [x_1, \ldots, x_n, x_{n+1}, \ldots, x_{n+N}]^T$$

Then define on each interval

$$\frac{i}{N + 1} < \tau \leq \frac{i + 1}{N + 1}$$

$$\hat{L}(\hat{x}, u, \tau) = (N + 1)(x_{n+i+1} - x_{n+i})L(x, u, t(\tau))$$

We can rewrite the functional (4) as

$$J = \phi(\hat{x}(1)) + \int_0^{\frac{1}{N+1}} \hat{L}(\hat{x}, u, \tau)\, d\tau + \cdots + \int_{\frac{N}{N+1}}^1 \hat{L}(\hat{x}, u, \tau)\, d\tau$$

$$= \phi(\hat{x}(1)) + \int_0^1 \hat{L}(\hat{x}, u, \tau)\, d\tau \qquad (6)$$

and the task is to minimize J in the extended state space, subject to the parameterized system given in Eq. (5), and to the corresponding path

2

constraints in Eq. (3). The new equivalent problem is a conventional optimal control problem. The last N components of the optimal solution of this problem, $\hat{x}^*$, will be the optimal switching times t_i for $i = 1, \ldots, N$.

III. Case Study

We consider a three-degree-of-freedom dynamic model that describes the point variable-mass motion of the aircraft over a flat-Earth model. We consider the vertical motion of the aircraft. A standard atmosphere is defined with $\Delta T_{\text{ISA}} = 0$. C_L is, in general, a function of the angle of attack and the Mach number: i.e., $C_L = C_L(\alpha, M)$. The lift coefficient is used as a variable rather than the angle of attack. We assume a parabolic drag polar: i.e., $C_D = C_{D_0} + K C_L^2$.

These hypotheses lead to the following set of differential algebraic equations (DAEs) for aircraft performance:

$$m\dot{V} = T - D - mg \sin\gamma, \qquad mV\dot{\gamma} = L - mg\cos\gamma$$

$$\dot{x} = V\cos\gamma, \qquad \dot{h} = V\sin\gamma, \qquad \dot{m} = -\eta T \qquad (7)$$

where T and C_L are the control inputs, and V, x, h, γ, and m are the state variables.

Given a commercial flight profile as a sequence of phases, initial and final conditions, and a set of path constraints, our goal is to find the minimum-fuel-consumption trajectory of the aircraft. Optimal switching times between phases and total flight time are also to be determined. The seven-phase flight profile used for the numerical simulation with its corresponding aerodynamic configurations and the operative procedures are given in Table 1. Note that according to our purpose of planning more efficient flight profiles within the current ATM paradigm, just one procedure per phase has been defined and the constant value of performance has been left free.

The characteristics of an Airbus A-320 have been taken from the Base of Aircraft Data (BADA) database.[§] The different aerodynamic configurations, the corresponding thresholds of use, and the value of the aerodynamic parameters are listed in Table 2. The boundary conditions of the flight are the following: $x_{t_I} = 0$, $h_{t_I} = 0$, $v_{t_I} = 115$ m/s, $\gamma_{t_I} = 0.1$ rad, $m_{t_I} = m_{\text{max}} = 77,000$ kg; $x_{t_F} = 2000$ km, and $h_{t_F} = 0$.

The path constraints of the problem are those that conform the aircraft's flight envelope and have been taken from the BADA database manual [20]. CL_{max_i} and V_{stall_i}, for $i = 1, \ldots, 7$, vary depending on the aerodynamic configuration. The rest of the constraints are equal for all phases:

$$0 \le h \le \min[h_{M0}, h_u], \qquad C_{V_{\text{min}}} V_{\text{stall}_i} \le V \le V_{Mo}$$

$$M \le M_{M0}, \qquad m_{\text{min}} \le m \le m_{\text{max}}, \qquad 0 \le C_L \le C_{L_{\text{max}_i}}$$

$$T \le T_{\text{max}}, \qquad \dot{m}_{\text{min}} \le \dot{m} \qquad (8)$$

where

$$h_u = h_{\text{max}} + G_t(\Delta T_{\text{ISA}} - C_{Tc,4}) + G_W(m_{\text{max}} - m)$$

and $C_{V_{\text{min}}} = 1.2$. Regarding the landing phase, γ has also been constrained according to the typical values of an aircraft's final descent path: i.e.,

$$-6 \text{ deg} \le \gamma_{\text{landing}} \le -3 \text{ deg} \qquad (9)$$

The reformulated optimal control problem is stated as follows:

$$\min J = \int_0^{\frac{1}{N+1}} \hat{L}(\hat{x}, u, \tau) \, d\tau + \cdots + \int_{\frac{N}{N+1}}^1 \hat{L}(\hat{x}, u, \tau) \, d\tau \qquad (10)$$

Subject to dynamic constraint

Table 1 Flight profile

Phase	Name	Configuration	Procedure
1	Takeoff	TO	$\gamma = c_1$ [a]
2	Initial climbing	IC	$\gamma = c_2$
3	Climb	CR	$V_{\text{CAS}} = c_3$
4	Cruise	CR	$h = c_4$
5	Descent	CR	$M = c_5$
6	Approach	AP	$M = c_6$
7	Landing	LD	$\gamma = c_7$

[a]With c_i, for $i = 1, \ldots, 7$, being undetermined constant values.

Table 2 A-320 aerodynamic configurations

Configuration	Flap	$C_{L_{\text{max}}}$	Threshold, ft[a]	CD_0	K
TO	1 + F	1.48	400	0.0393	0.0396
IC	1	1.35	2000	0.0242	0.0469
CR	Clean	1.17	-	0.024	0.0375
AP	2	1.84	8000	0.0456	0.0381
LD	Full	1.88	3000	0.0838	0.0371

[a]Threshold altitude for configuration change.

$$x' = (N + 1)(x_{n+i+1} - x_{n+i})\hat{f}_i(x, u, \tau) \qquad (11)$$

switching dynamic constraint

$$x'_{n+1} = \cdots = x'_{n+N} = 0 \qquad (12)$$

initial boundary condition

$$x(t_I) = x_{t_I} \qquad (13)$$

final boundary condition

$$\psi(x(t_F), t_F) = 0 \qquad (14)$$

and path constraints

$$\phi_{l_i} \le \phi_i[x, u] \le \phi_{u_i} \qquad (15)$$

where $i = 1, \ldots, 7$ corresponds to the sequence of phases of the flight given in Table 1, $N = 6$ is the number of switches, and $\hat{L}(\hat{x}, u, \tau) = m'$. Equation (11) corresponds to the aircraft DAE system given in Eq. (7), parametrized and particularized to the dynamic mode of each phase. Equation (12) are dynamic constraints associated to the switching variables. Equations (11) and (12) constitute the DAE system for the extended vector $\hat{x}$ and Eqs. (13) and (14) are the initial and final conditions. Finally, Eq. (15) corresponds to the set of constraints of each phase given in Eqs. (8) and (9).

To solve the optimal control problem (10–15) a Simpson collocation method [15,16] has been used. The resulting sparse nonlinear programming problem (NLP), has been solved using IPOPT [21]. It had 1795 variables, 1525 equality constraints, and 1599 inequality constraints. The total computational time on a 2.56 GHz laptop with 4 GB RAM was 80.9005 s, showing the high computational efficiency of the method.
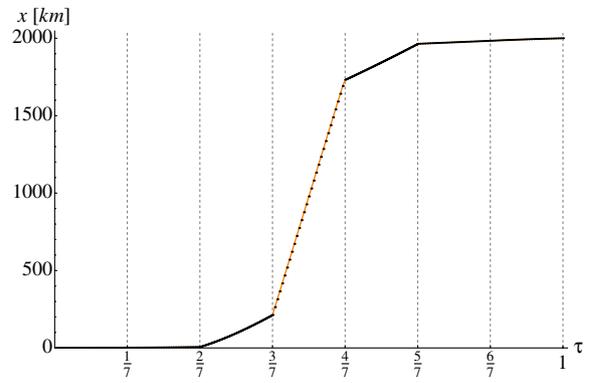
Table 3 Results

Phase	Switches, s	Consumption, kg	Value
Takeoff	11.00	22.63	γ given [a]
Initial climbing	50.43	104.951	γ given
Climb	1186.16	1502.27	$V_{\text{CAS}} = 129.57$ m/s
Cruise	7498.67	4728.21	$h = 10,780.1$ m
Descent	8924.89	4896.79	$M = 0.52$
Approach	9037.08	4912.26	$M = 0.52$
Landing	9162.37	4930.51	$\gamma = -3.24$ deg

[a]Given by the initial condition.

3

a) τ-h
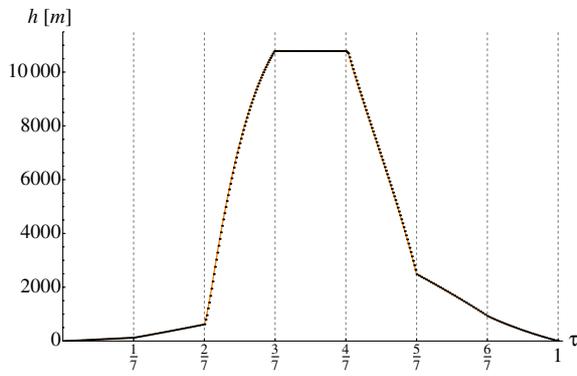
b) τ-x
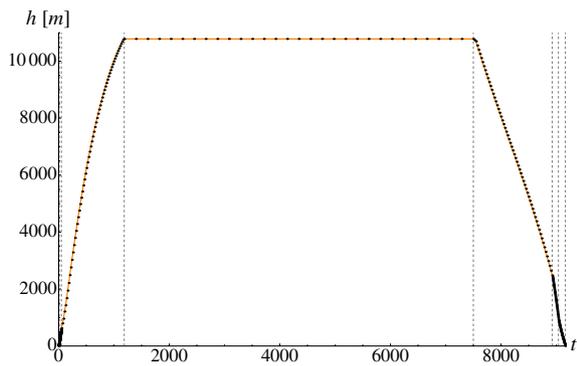
c) t-h
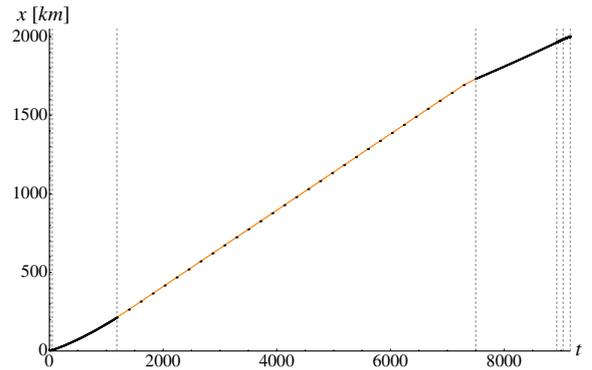
d) t-x

Fig. 2   Altitude *h* and distance *x*.

a) τ-V
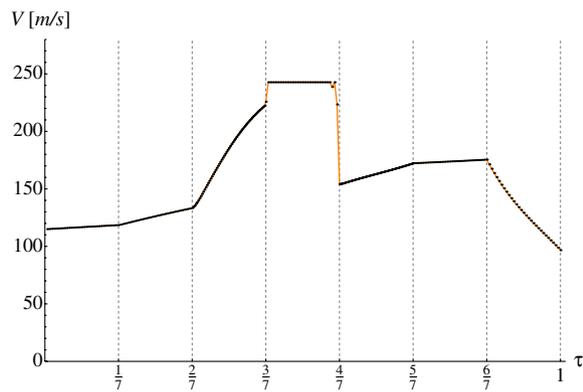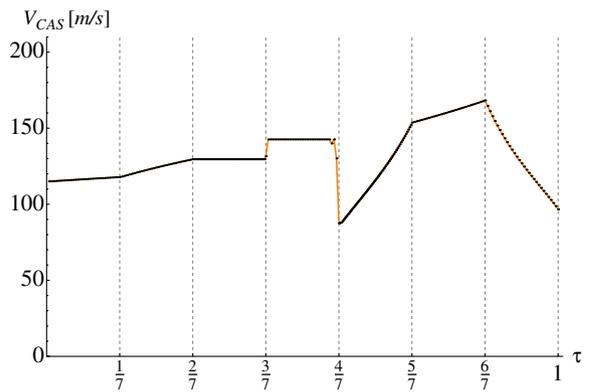
b) τ-V_{CAS}
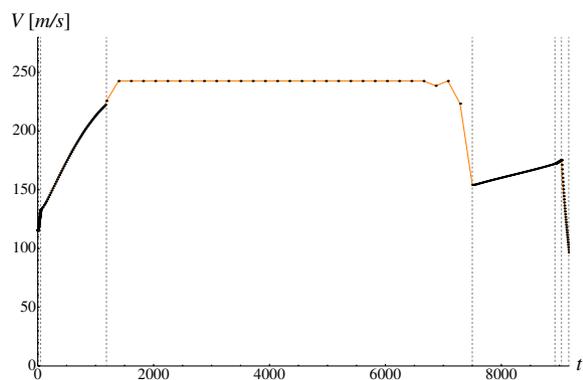
c) t-V
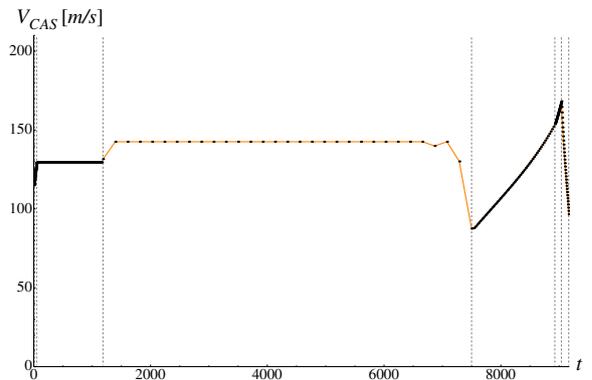
d) t-V_{CAS}

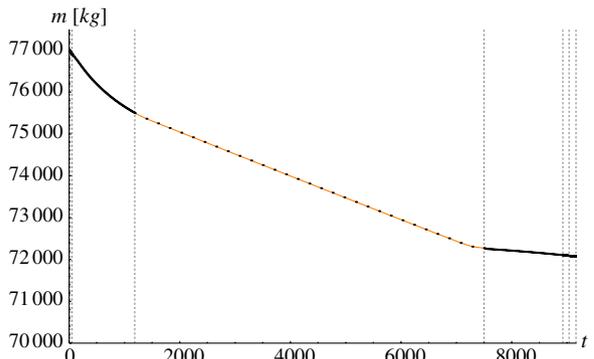**Fig. 3   True airspeed *V* and calibrated airspeed V_{CAS}.**

4

a) τ–γ

b) τ–m

c) t–γ
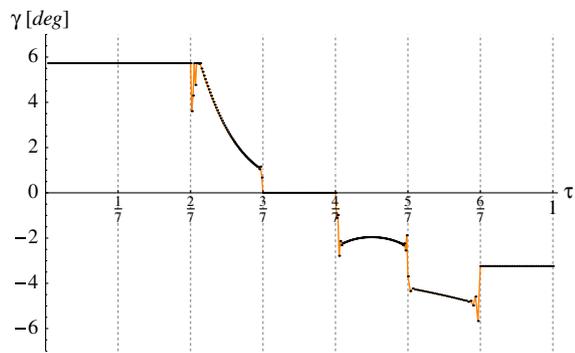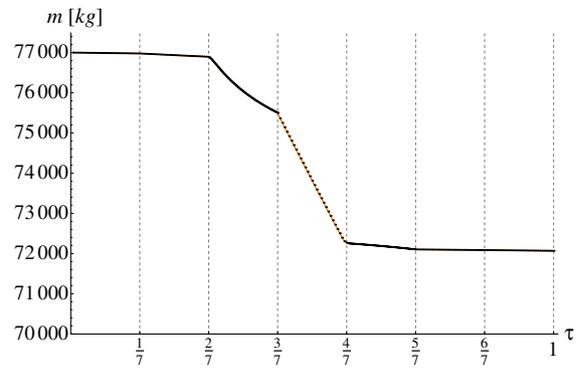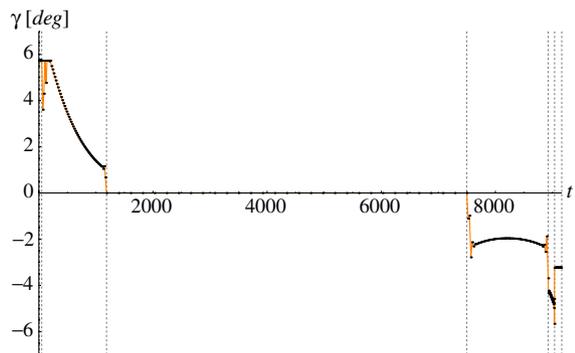
d) t–m

Fig. 4   Aircraft mass *m* and flight-path angle *γ*.

a) τ–C_L
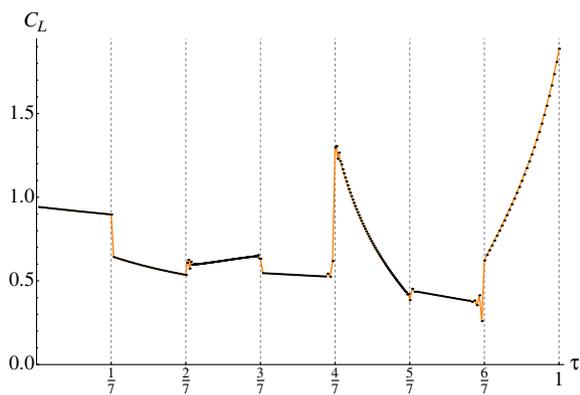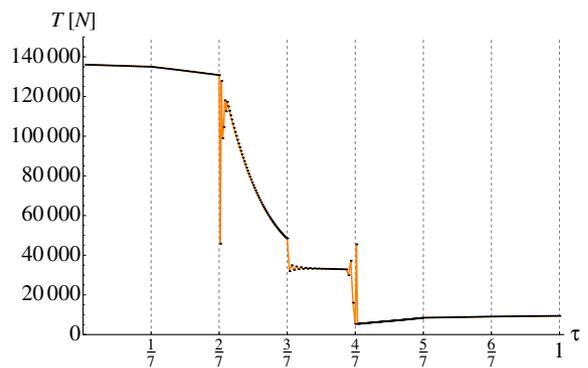
b) τ–T
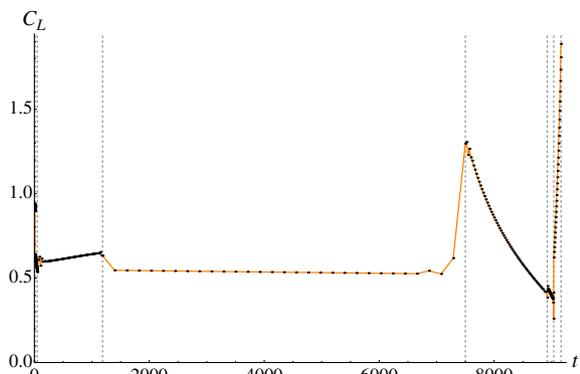
c) t–C_L
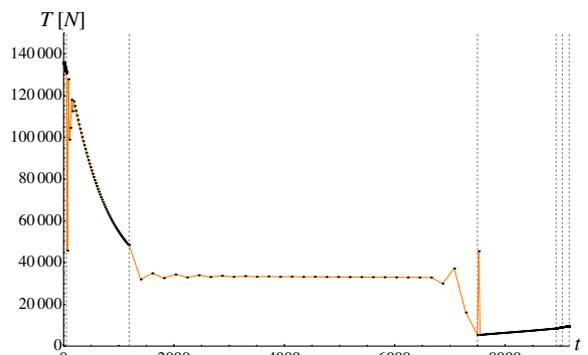
d) t–T

Fig. 5   Control laws.

Table 4   Results of backward integration

States	Value at t_I (backward integration)	Exact value at t_I
h	1.3361×10^{-3}	0
x	1.7473×10^{-1}	0
γ	0.9809	1
v	0.9489	1
m	0.9929	1

A. Results

Table 3 shows the six switching times between phases and the total flight time (9162.37 s), the accumulated consumption at the end of every phase (4930.51 kg total consumption), and the constant values that describe aircraft performance in the different flight procedures. These values are also part of the optimal solution.

The optimal control law, the optimal switching instants, and the evolution of the state variables are represented in Figs. 2–5. For the sake of clarity, both control inputs and state variables are represented in terms of scaled time τ and in terms of real time t. Scaled time τ ranges from 0 to 1. A discretization grid has been defined for τ with $n = 270$: phases 1, 2, 4, 6, and 7 with $n_i = 30$ and phases 3 and 5 with $n_i = 60$.

In Figs. 2–5 the seven phases are clearly distinguishable in both timescales. Switches between phases 1–2, 2–3, 5–6, and 6–7 are autonomous; i.e., they occur when the aircraft reaches the respective threshold altitudes. On the contrary, switches between phases 3–4 and 4–5 are controlled, since they are given by the control law within the optimal solution. Both the cruise altitude and the starting point of descent (respectively, switches 3 and 4) are not prefixed, but are set by the optimal solution, leading the system to the overall minimum fuel consumption.

Figures 2–4 show the state variables. In general, except for the case of γ (Fig. 4), all state variables vary smoothly, and γ exhibit high-frequency dynamics in phases 3 and 5, but are within reasonable values for aircraft performance. Figure 5 shows the expected behavior of control inputs.

B. A Posteriori Verification

Direct-transcription methods do not use the calculus of variations first-order necessary conditions [22]. However, it has been demonstrated that Karush–Khun–Tucker NLP necessary conditions approach the optimal control necessary conditions as the number of variables grows [23].

Therefore, we first mapped the discrete solution to the continuous domain using spline polynomials. The continuous control and state variables satisfy the normalized dynamic equations with a tolerance between 10^{-4} and 10^{-6} in most of the time domain. However, in small intervals close to the switching times they are not fulfilled, due to spurious wiggles in the interpolant polynomial.

Additionally, it is necessary to check that our solution fulfills the calculus of variations first-order necessary conditions. For this purpose, we compared the direct-transcription solution with the first-order necessary conditions [24]. We used the final values of states and costates obtained from the direct solution to backward integrate the state and costate dynamics together with the control algebraic equations. If initial state x_I is accurately recovered, the first-order necessary conditions are fulfilled, thus verifying the optimality of the direct-transcription discrete solution (see [16,25] for more details).

Using this procedure, we recovered the normalized initial state, as shown in Table 4.

IV. Conclusions

The hybrid optimal control approach herein presented provides an overall optimal solution for a realistic seven-phase complete flight in which total fuel-consumption is minimized and switching times are obtained within the extended problem. We show that another concept of operation in air traffic management is possible, planning more efficient flight profiles toward cost-effectiveness, environmental sustainability, and, at the same time, meeting safety requirements.

References

[1] Lygeros, J., Sastry, S., and Tomlin, C., "The Art of Hybrid Systems," *Compendium of Lecture Notes for the Hybrid Systems Class*, Univ. of California, Berkeley, Berkeley, CA, 2002, pp. 231–248..

[2] Branicky, M. S., Borkar, V. S., and Mitter, S. K., "A Unified Framework for Hybrid Control: Model and Optimal Control Theory," *IEEE Transactions on Automatic Control*, Vol. 43, No. 1, 1998, pp. 31–45. doi:10.1109/9.654885

[3] Ross, I. M., and D'Souza, C. N., "Hybrid Optimal Control Framework for Mission Planning," *Journal of Guidance, Control, and Dynamics*, Vol. 28, No. 4, July–Aug. 2005, pp. 686–697. doi:10.2514/1.8285

[4] Xu, X., and Antsaklis, P. J., "Optimal Control of Switched Systems via Nonlinear Optimization Based on Direct Differentiations of Value Functions," *International Journal of Control*, Vol. 75, No. 16/17, 2002, pp. 1406–1426. doi:10.1080/0020717021000023825

[5] Xu, X., and Antsaklis, P. J., "Results And Perspectives on Computational Methods for Optimal Control of Switched Systems," *Hybrid Systems: Computation and Control*, Springer, New York, 2003, pp. 540–555.

[6] Roh, W., and Kim, Y., "Trajectory Optimization for a Multi-Stage Launch Vehicle Using Time Finite Element and Direct Collocation Methods," *Engineering optimization*, Vol. 34, No. 1, 2002, pp. 15–32. doi:10.1080/03052150210912

[7] Huntington, G. T., and Rao, A. V., "Optimal Configuration of Spacecraft Formations via a Gauss Pseudospectral Method," *Advances in the Astronautical Sciences*, Vol. 120, 2005, pp. 33–50.

[8] Jorris, T. R., and Cobb, R. G., "Multiple Method 2-D Trajectory Optimization Satisfying Waypoints and No-Fly Zone Constraints," *Journal of Guidance, Control, and Dynamics*, Vol. 31, No. 3, May–June 2008, pp. 543–553. doi:10.2514/1.32354

[9] Jorris, T. R., and Cobb, R. G., "Three-Dimensional Trajectory Optimization Satisfying Waypoints and No-Fly Constraints," *Journal of Guidance, Control, and Dynamics*, Vol. 32, No. 2, March–April 2009, pp. 551–572. doi:10.2514/1.37030

[10] Benson, D., "A Gauss Pseudospectral Transcription for Optimal Control," Ph.D. Thesis, Dept. of Aeronautics and Astronautics, Massachusetts Inst. of Technology, Cambridge, MA, 2004.

[11] Fahroo, F., and Ross, I. M., "Direct Trajectory Optimization by a Chebyshev Pseudospectral Method," *Journal of Guidance, Control, and Dynamics*, Vol. 25, No. 1, Jan.–Feb. 2002, pp. 160–166. doi:10.2514/2.4862

[12] Ross, I. M., and Fahroo, F., "Pseudospectral Knotting Methods for Solving Optimal Control Problems," *Journal of Guidance, Control, and Dynamics*, Vol. 27, No. 3, May–June 2004, pp. 397–405. doi:10.2514/1.3426

[13] Xu, X., and Antsaklis, P. J., "Optimal Control of Switched Systems Based on Parameterization of the Switching Instants," *IEEE Transactions on Automatic Control*, Vol. 49, No. 1, 2004, pp. 2–16. doi:10.1109/TAC.2003.821417

[14] Žefran, M., "Continuous Methods for Motion Planning," Ph.D. Thesis, Univ. of Pennsylvania, Computer and Information Science, PA, Philadelphia, 1996.

[15] Hargraves, C. R., and Paris, S. W., "Direct Trajectory Optimization Using Nonlinear Programming and Collocation," *Journal of Guidance, Control, and Dynamics*, Vol. 10, No. 4, July–Aug. 1987, pp. 338–342. doi:10.2514/3.20223

[16] Herman, A. L., and Conway, B. A., "Direct Optimization Using Collocation Based on High-Order Gauss-Lobatto Quadrature Rules," *Journal of Guidance, Control, and Dynamics*, Vol. 19, No. 3, May–June 1996, pp. 592–599.

doi:10.2514/3.21662

[17] Betts, J. T., and Cramer, E. J., "Application of Direct Transcription to Commercial Aircraft Trajectory Optimization," *Journal of Guidance, Control, and Dynamics*, Vol. 18, No. 1, Jan.–Feb. 1995, pp. 151–159.
doi:10.2514/3.56670

[18] Wu, D., and Zhao, Y. J., "Performances And Sensitivities Of Optimal Trajectory Generation for Air Traffic Control Automation," AIAA Guidance, Navigation, and Control Conference, AIAA Paper 2009-6167, 10–13 Aug. 2009.

[19] Pargett, D. M., and Ardema, M. D., "Flight Path Optimization at Constant Altitude," *Journal of Guidance, Control, and Dynamics*, Vol. 30, No. 4, July–Aug. 2007, pp. 1197–1201.
doi:10.2514/1.28954

[20] Nuic, A., *User Manual for the Base of Aircraft Data (BADA)* Rev. 3.6, Eurocontrol Experimental Center, Brétigny-sur-Orge, France, 2005.

[21] Kawajir, Y., Laird, C., and Wachter, A., *Introduction to IPOPT: A Tutorial for Downloading, Installing, and Using IPOPT* [online document], 2006, http://www.coin-or.org/Ipopt/documentation/ [retrieved 15 Mar. 2010].

[22] Bryson, A. E., and Ho, Y. C., *Applied Optimal Control*, Wiley, New York, 1975, pp. 90–125.

[23] Betts, J. T., and Kolmanovsky, I., "Practical Methods for Optimal Control Using Nonlinear Programming," *Applied Mechanics Reviews*, Vol. 55, No. 4, 2002, pp. 81–132.

[24] Yan, H., Fahroo, F., and Ross, I. M., "Accuracy and Optimality of Direct Transcription Methods," *Advances in the Astronautical Sciences*, Vol. 105, No. ??, 2000, pp. 1613–1630.

[25] Scheel, W. A., and Conway, B. A., "Optimization of Very-Low-Thrust, Many-Revolution Spacecraft Trajectories," *Journal of Guidance, Control, and Dynamics*, Vol. 17, No. 6, Nov.–Dec. 1994, pp. 1185–1185.
doi:10.2514/3.21331